Fast Frequency Response for Effective Frequency Control in Power Systems with Low Inertia

Qiteng Hong[1], Marcel Nedd[1], Seán Norris[2], Ibrahim Abdulhadi[1], Mazaher Karimi[3,5], Vladimir Terzija[3], Benjamin Marshall[4], Keith Bell[1], Campbell Booth[1]*

[1]*University of Strathclyde, 99 George Street, G1 1XW, Glasgow, UK*
[2]*GE Power, Tanfield, Edinburgh, EH3 5DA, UK*
[3]*University of Manchester, Oxford Rd, Manchester, M13 9PL, UK,*
[4]*National Grid, Warwick, CV34 6DA, UK*
[5]*Gonbad Kavous University, Iran*
**q.hong@strath.ac.uk*

Keywords: Low inertia, frequency control, wide-area monitoring and control, PMUs, renewable generation

Abstract

The increasing penetration of renewable generation has led to the decrease of power systems' overall inertia, which introduces significant challenges to frequency stability. In this paper, the potential of using Fast Frequency Response (FFR) to enhance frequency control in power systems with low inertia is investigated in detail. A Generic System Frequency Response (GSFR) model taking into account of the penetration level of Non-Synchronous Generation (NSG) and FFR has been developed and used to investigate the impact of reduced inertia on frequency control and demonstrate that the amount of reserve power to be scheduled can be significantly reduced with the deployment of FFR. The impact of the different FFR resources' characteristics (e.g. response delay, ramp rate, etc.) on the effectiveness of frequency control is also investigated, based on which the desirable specifications for FFR schemes are summarised. These desirable properties of FFR schemes are taken into account in the design of a wide-area monitoring and control system termed "Enhanced Frequency Control Capability (EFCC)", which is proposed for the delivery of FFR in the future Great Britain transmission system. The design and operation of the EFCC scheme are presented, along with a case study demonstrating its effectiveness in enhancing the frequency control.

1. Introduction

In the Great Britain (GB) power system, a significantly increased level of renewable generation has been integrated in the past several years and this trend is expected to continue in the coming decades [1]. Renewable energy resources are mostly interfaced with the network through converters, which do not naturally provide inertia. Therefore, the increased penetration of renewables could lead to the decrease in the overall system inertia if no mitigating measures are taken [2]. This will pose significant operational challenges as for the same amount of power imbalance, a lower system inertia will lead to a higher Rate of Change of Frequency (RoCoF). As a result, the system operator (and automatic control schemes) will have less time to respond to disturbances and avoid the frequency deviating beyond the required limits.

At present, the containment of frequency deviations from the nominal is mainly achieved by primary response through turbine governor control [3]. In GB, primary response is required to be activated within 2 s following a frequency event and is expected to provide full response within 10 s and sustain it for 20 s [1]. It is required that the frequency should be maintained within the statutory limit between 49.5 Hz and 50.5 Hz [4]. With the decrease of system inertia, conventional primary responses may not be fast enough to maintain the frequency within required levels in the immediate aftermath of disturbances and the frequency may drop below the acceptable limit before the primary response injects sufficient additional power into the system.

One of the most promising solutions for effective control of frequency in a low-inertia system is to provide faster frequency response than the conventional primary response [5]. In this paper, the term Fast Frequency Response (FFR) specifically refers to frequency response schemes that can be triggered within 1 s and the use of FFR to tackle the frequency control challenges in a system with low inertia is investigated in detail. A Generic System Frequency Response (GSFR) model based on the model reported in [6] has been developed to further consider the impact of the penetration of Non-Synchronous Generation (NSG) and the incorporation of FFR on frequency behaviour during power imbalance events. The model has been used to demonstrate the impact of reduced inertia on frequency behaviour and the significant increase in reserve primary response capacity required to maintain the frequency within acceptable limits. The model is also used to demonstrate that by deploying FFR, the frequency can be controlled sufficiently effective with a significantly lower reserve capacity.

In this paper, the impact of the characteristics of the resources' capability in delivering FFR (e.g. response delay, ramp rate, capacity, etc.) is also investigated. The outcomes of these studies inform the desirable specifications of systems providing FFR services. The paper then presents an FFR scheme that takes all these desirable specifications into account in its design. This FFR scheme is termed "Enhanced Frequency Control Capability (EFCC)" [5], which uses wide-area monitoring and control techniques for detecting frequency events and deploying coordinated responses from a variety of resources (e.g. energy storage, wind, demand, etc.). The design and operation of the EFCC scheme will be presented, along with a case study demonstrating its effectiveness in enhancing the frequency control.

The paper is organized as follows: in Section 2, the GSFR model is presented and used to demonstrate advantages in introducing FFR. Section 3 presents the impact of the characteristics of the FFR resources on the effectiveness of

frequency control. Section 4 presents the design and operation of the EFCC scheme for delivering FFR. In Section 5, a case study that demonstrates the effectiveness of the EFCC scheme in enhancing the frequency control is presented.

2. Advantages in introducing faster frequency response

2.1. Generic System Frequency Response model

A System Frequency Response (SFR) model has been developed for estimating the frequency behaviour during power imbalance events [6]. However, the SFR model described in [6] is designed for systems that are dominated by reheated steam turbine generators, which makes it less applicable for systems with increasing penetration of NSG. Therefore, in this paper a generic SFR (GSFR) model has been developed, which considers the NSG penetration level and can be used for investigating the impact of introducing FFR on frequency behaviour during power imbalance disturbances. The GSFR model is shown in Fig. 1 and a description of the associated parameters is provided in Table 1.

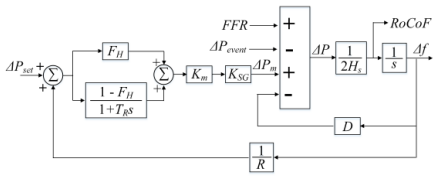

Fig. 1. Generic System Frequency Response (GSFR) model

In this GSFR model, a simplification has been made, where the overall system inertia I_s is contributed by two main sources, i.e. synchronous generation and the demand side (e.g. distribution connected generation, motors, etc.). The overall system inertia can be calculated as follows (a description of the associated parameters is provided in Table 1):

$$I_s = \sum H_{SG}^i S_{SG}^i + \overline{H_{DM}} S_{DM} \quad (1)$$

Using an equivalent average inertia constant $\overline{H_{SG}}$ and rated apparent power S_{SG}^T to represent the inertia contribution from synchronous generators lead to (2):

$$I_s = \overline{H_{SG}}\, S_{SG}^T + \overline{H_{DM}} S_{DM} \quad (2)$$

where:

$$S_{SG}^T = \frac{P_{DM} K_{SG}}{K_{LF} K_{PF}} \quad (3)$$

$H_{DM} S_{DM}$ represents the inertia contribution from the demand. Based on the consultation with experienced engineers in GB transmission network operator, S_{DM}, which is the base for evaluating the demand equivalent inertia constant, is commonly chosen as P_{DM} , i.e. $S_{DM} = P_{DM}$. It should be noted that a different S_{DM} can also be chosen, which will result in a different equivalent $\overline{H_{DM}}$, but the total kinetic energy stored in the demand will not change, hence it will not change the frequency behaviour simulated by the GSFR model.

The overall system inertia can be then represented in (4):

$$I_s = \frac{\overline{H_{SG}}\, P_{DM} K_{SG}}{K_{LF} K_{PF}} + \overline{H_{DM}}\, P_{DM} \quad (4)$$

Using the rated apparent power of the overall system as the base, i.e.:

$$S_{base} = \frac{P_{DM}}{K_{LF} K_{PF}} \quad (5)$$

the overall system equivalent inertia constant can be derived in (6), from which it can be seen that the overall system inertia constant is directly affected by the factor K_{SG} , which is the fraction of synchronous generation in the generation mix. System inertia is also affected by the average inertia constant of the synchronous generators $\overline{H_{SG}}$ that are operating (reflecting the size of the machines contributing to the inertia) and the demand $\overline{H_{DM}}$.

$$\begin{aligned} H_s &= \frac{I_s}{S_{base}} \\ &= \frac{\frac{\overline{H_{SG}}\, P_{DM} K_{SG}}{K_{LF} K_{PF}} + \overline{H_{DM}}\, P_{DM}}{\frac{P_{DM}}{K_{LF} K_{PF}}} \\ &= \overline{H_{SG}}\, K_{SG} + \overline{H_{DM}}\, K_{LF} K_{PF} \end{aligned} \quad (6)$$

Table 1. Description of parameters used in the study

Parameter	Description
ΔP_{set}	Change of synchronous generators' power set point in p.u.
F_H	Fraction of power generated by the turbine
T_R	Reheat time constant in seconds
K_m	Mechanical power gain factor
K_{PR}	Fraction of synchronous generators providing primary response
K_{SG}	Fraction of synchronous generators' contribution to overall demand
ΔP_m	Change of mechanical power output in p.u.
ΔP_{event}	Power imbalance in p.u. (the value is positive for loss of generation events)
ΔP	Overall power imbalance in p.u.
R	Regulation constant for droop control
H_s	System equivalent inertia constant in seconds
I_s	Overall system equivalent inertia in GVAs
$\overline{H_{SG}}$	Overall equivalent inertia constant of synchronous generators in seconds
$\overline{H_{DM}}$	Overall equivalent inertia constant of demand in seconds
H_{SG}^i	Individual synchronous generator's inertia constant
S_{SG}^i	Individual synchronous generator's capacity
S_{SG}^T	Total capacity of on-line synchronous generators
S_{base}	The base for evaluating system equivalent inertia constant
P_{DM}	Active power demand
K_{LF}	Loading factor
K_{PF}	Power factor

This GSFR model has been tuned to replicate a historical loss of infeed event in the GB transmission system. The generation mix of the event is shown in Table 2 and the tuned parameters of the model are provided in Table 3. The comparison of the simulated and actual frequency profiles is shown in Fig. 2, where it can be seen that the model has accurately replicated the event. It should be noted that although the results show a high-level of accuracy in representing this particular event, a number of assumptions have been made. For example, the average $\overline{H_{SG}}$ is assumed to be 5 s; and the loading factor K_{LF} and power factor K_{PF} are assumed to be 0.8 and 0.85 respectively. These assumptions are made based on a simplified GB transmission system model that is widely used for research [7]. The exact values for these parameters in the actual system could be different from these values. Nevertheless, this case is still considered to be useful as a base case for investigating the impact of decreased inertia and the incorporation of FFR on the frequency profile.

Table 2. System operating condition of the historical event on 11th Jan 2016 [8]

Demand	28.27 GW
Loss of infeed	1 GW
Coal	4.83 GW
Nuclear	6.73 GW
CCGT	7.44 GW
Interconnector	3.44 GW
Hydro	0.48 GW
Biomass	2.08 GW
Wind	3.30 GW

Table 3. Parameter values for the GSFR model

Parameter	**Value**
R	0.05
K_{SG} (%)	76.2%
K_{PR} (%)	32.2%
$\overline{H_{SG}}$	5 s
$\overline{H_{DM}}$	1.83 s
K_{LF}	0.8
K_{PF}	0.85
F_H	0.1
T_R	8 s
ΔP_{event}	1 GW (need to convert to p.u. in the model)
Initial frequency	49.981 Hz

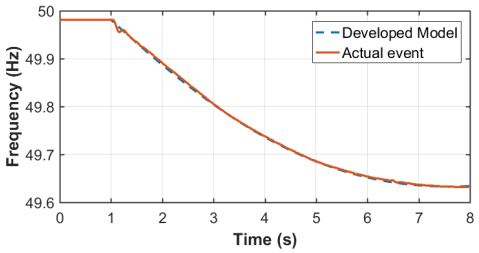

Fig. 2. Simulated and actual frequency profile

2.2. *Impact of decreased system inertia on frequency control*

The GSFR model presented in Section 2.1 has been used for simulating a number of cases shown in Table 4. The values are chosen to approximately represent the GB system with highest to lowest inertia between 2016 and 2017 as reported in [1]. The simulated event is a loss of 1.32 GW generation, which is assumed to be the largest generation loss in the GB system [9, 10]. Case 1 represents a high-inertia scenario, where 80% of the generation is provided by synchronous generation, and with the primary response provided by 23.6% of the spinning reserve capacity, the frequency nadir can be maintained just at the required 49.5 Hz level as shown in Fig. 3. As the inertia decreases in Case 2 and Case 3 due to the higher penetration of NSG and lower demand condition, the same event will result in much lower frequency nadir. In Case 3, when the system has low demand and low inertia, which usually occurs during a sunny summer day in the UK, the frequency nadir can fall below 49.3 Hz for the same event.

To cater for such poor frequency behaviour, in Case 4, the primary response reserve has been increased from 23.6% to 43.2%, which maintains the frequency nadir at 49.5 Hz. However, this represents 43.2% - 23.6% = 19.6% (equivalent to 2.31 GVA with $S_{SG}^{T} = 11.75\ GVA$) increase in reserve synchronous generation capacity for primary response, which leads to a significant increase in operational cost.

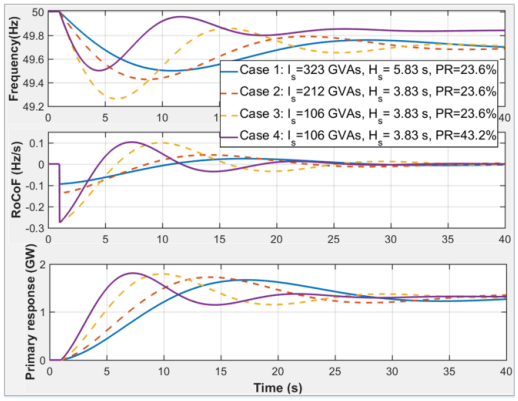

Fig. 3. Simulation results demonstrating the impact of reduced inertia on frequency behaviour

Table 4. Cases for the investigation of the impact of reduced inertia on frequency behaviour

	Case 1	**Case 2**	**Case 3**	**Case 4**
Demand (GW)	40	40	20	20
K_{SG} (%)	80	40	40	40
K_{PR} (%)	23.6	23.6	23.6	43.2
I_s (GVAs)	323	212	106	106
H_s (s)	5.83	3.83	3.83	3.83

2.3. *Fast frequency response to enhance frequency control*

In this study, the FFR is incorporated into the system. The FFR is modelled as a ramp up function as shown in Fig. 4.

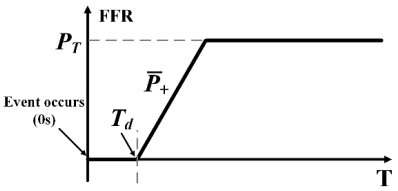

Fig. 4. Characteristics of the modelled FFR

To investigate how FFR can facilitate the frequency control, the cases listed in Table 5 are studied. Case 1 is used as the base case, where the system has relatively high inertia, while Case 2 represents the scenario where the system has very low inertia due to low demand and high NSG penetration level. In Case 3, additional primary response has been used to maintain frequency limit of 49.5 Hz, while in Case 4, the FFR is used to facilitate frequency restoration without increasing the amount of primary response reserve in relation to Cases 1 and 2. The results of the simulation are shown in Fig. 5.

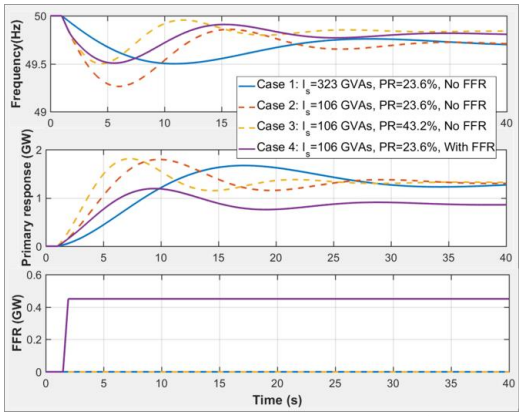

Fig. 5. Simulation results illustrating the use of FFR to enhance frequency control

Table 5. Cases for investigation of deploying FFR to enhance frequency control

	Case 1	Case 2	Case 3	Case 4
Demand (GW)	40	20	20	20
K_{SG} (%)	80	40	40	40
K_{PR} (%)	23.6	23.6	43.2	23.6
I_s (GVAs)	323	106	106	106
H_s (s)	5.83	3.83	3.83	3.83
FFR	No	No	No	Yes

It can be seen that in Case 1, the system is capable of handling the frequency within the required limit with relatively low primary response reserve. However, with the same amount of primary response reserve, the frequency will drop to unacceptable level as shown in Case 2 due to the lower system inertia. In Case 3, the primary response has to be increased from 23.6% to 43.2% to maintain the same frequency nadir observed in Case 1. As presented in Section 2.2, this represents an additional 2.31 GVA of reserve capacity. In Case 4, the same low-inertia scenario as in Case 2 and 3 is simulated, but the primary response is kept as 23.6% while 450 MW of FFR is introduced. In this case, the FFR response delay T_d is assumed to be 0.5 s and the ramp up rate $\overline{P}_+$ is assumed to be 1000 MW/s. The results show that with this faster response, the frequency can be maintained as the same level as in Case 1 with much lower reserve capacity compared to Case 3. This shows that with faster frequency response, the reserve power can be significantly reduced.

3. Impact of FFR characteristics on the effectiveness of frequency control

In this section, the impact of the characteristics of FFR on the performance of frequency restoration is investigated. The cases used for investigation are provided in Table 6. Specifically, Case 0 is where no FFR is available. The following operation condition representing a low inertia scenario is used for study: P_{DM} = 20 GW, K_{SG} = 0.4, P_{event} = 1.32 GW, K_{PR} = 23.6%, and K_{LF} = 0.8.

Table 6. Cases for investigate the impact of FFR characteristics

Case	T_d (s)	$\overline{P_+}$ (MW/s)	P_T (MW)
0	No FFR		
1	0.3	1000	500
2	0.5	1000	500
3	0.8	1000	500
4	1	1000	500
5	0.3	600	500
6	0.3	400	500
7	0.3	200	500
8	0.3	100	500
9	0.3	1000	200
10	0.3	1000	600
11	0.3	1000	1000
12	0.3	200	1000

3.1. *Impact of FFR response delay (T_d)*

The response delay of FFR is mainly dominated by the delay in detecting the frequency event and the response of the resource due to its capability. The detection delay could be as a result of communication latency, intentionally introduced dead band to avoid mal-operation, etc. Fig. 6. shows the simulation results with different response delays under the same FFR capacity and ramp up rate.

From Case 1 to Case 4, the detection delay is gradually increased from 0.3 s to 1 s. It can be seen from Fig. 6 that the changes in frequency nadir are not significant. This means that if the resource's ramp up rate $\overline{P}_+$ and the capacity P_T is sufficiently high, the impact of the detection delay (up to 1 s, which is considered to be sufficient for detecting frequency events) does not appear to be significant.

This can be explained as follows: if an event causes a maximum RoCoF of 0.125 Hz/s, it takes 4 s for the frequency to drop to 49.5 Hz. In a more severe case where the RoCoF is doubled, i.e. 0.25 Hz/s, it takes 2 s for the frequency to drop to 49.5 Hz. Therefore, theoretically, if the FFR can be ramped up sufficiently high and with sufficient capacity, which can be achieved by resources like energy storage, the response delay within 1 s will not have significant impact on the overall effectiveness of the FFR scheme.

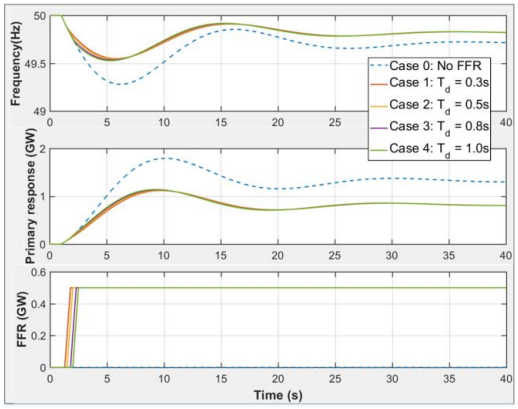

Fig. 6. Impact of FFR response delay on frequency behavior

3.2. *Impact of FFR ramp up rate ($\bar{P}_+$)*

The ramp up rate is mainly associated with the type of the resource providing the FFR. Energy storage resource and flexible demand can potentially change their power at a near-instantaneous time scale, while other resources like CCGTs are relatively slower. This section will investigate how the ramp up rate can affect the frequency behaviour during disturbances.

A range of cases with different ramp up rates have been studied and the results are shown in Fig. 7 and listed in Table 6. All the presented cases have the same response delay and capacity. Case 1 represents a scenario with highest ramp up rate. From Case 5 to Case 8 the ramp up rate is decreased from 500 MW/s to 100 MW/s. It can be seen from Fig. 7 that the effectiveness of the FFR in facilitating the frequency control has been significantly compromised with the decreased ramp up rate even with very short response delay (i.e. 0.3 s). This reveals the importance of speed of the resources in delivering the power they are required to provide. Clearly, the higher ramp-up rate is more preferable. This could be difficult for conventional large synchronous generators to achieve due to the nature of the machines, therefore resources such as energy storage, demand curtailment and HVDC interconnectors are more suited to the provision of FFR services.

3.3. *Impact of FFR capacity (P_T)*

This section investigates the impact of the capacity of the FFR on the frequency behaviour during disturbances. Case 9 to Case 12 as listed in Table 6 are used for the study. Cases 9 to 11 have the same ramp up rate and response delay, but the capacity is gradually decreased from 1000 MW to 200 MW. The simulated results are shown in Fig. 8, which shows that as the FFR capacity decreases, the frequency nadir tends to decrease. This is due to the decrease of FFR capacity making the system more reliant on the conventional primary response, which is relatively slower.

Cases 9 and 12 have the same high FFR capacity but Case 12 has lower ramp up rate. It can be seen that Case 12 has a much lower frequency nadir compared to Case 9. This is because even with sufficient capacity, Case 12 is slow in delivering the power, so the frequency would have already fallen below the required limit before the FFR resource fully delivers its power. This means that a high FFR capacity will only be effective with a sufficiently high ramp up rate.

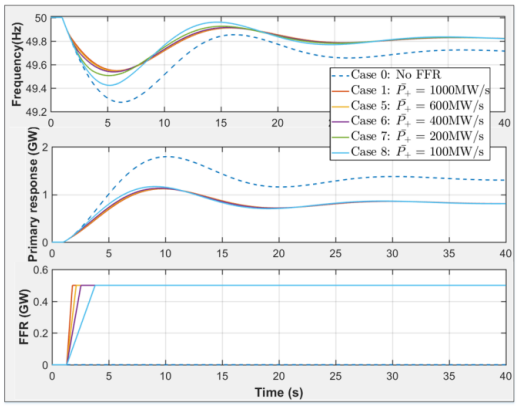

Fig. 7. Impact of ramp rate of the resource on frequency behaviour

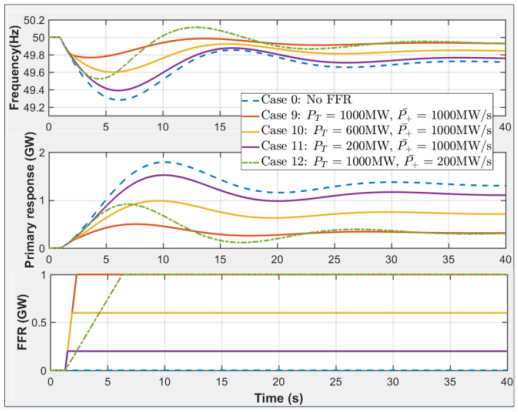

Fig. 8. Impact of the capacity of the FFR resource on frequency behaviour

3.4. *The need for regional frequency response*

From previous discussions, it is clear that a fast response to frequency disturbances is key to effectively maintaining the frequency within acceptable limits in future grids with low inertia. However, solely being fast to respond to the event may not be sufficient. In the real grid, it is common that different regions have different levels of available renewable resources, e.g. in the GB transmission network, Scotland has a relatively higher penetration of wind than the rest of GB. This will lead to regional variations of inertia (i.e. inertia values may be different at different locations of the network depending on the local generation mix). The nature of the network with regional variations in frequency has been reported in a number of publications [7, 11], and the conventional measure of overall system frequency may no longer apply effectively to current and future scenarios.

Therefore, it is important that a future FFR scheme possesses the capability to take the regional impact of disturbances into account to deploy a targeted the response for the restoration of frequency and maintenance of synchronism between different areas. Otherwise, it can lead to the response being less effective, or in the worst case, increase the chance of system separation, which may ultimately lead to blackout.

4. Enhanced Frequency Control Capability (EFCC) scheme

From the studies and discussions presented in Section 3, it is clear that FFR could potentially be an effective solution for frequency control in power systems with low inertia, and the desirable FFR scheme should be able to: coordinate the available resources to provide higher ramp up capability and suitable overall capacity; detect and react to the frequency event promptly; and the regional variation in inertia thus the frequency behaviour during disturbances should be considered.

In this section, an FFR scheme taking all these desirable specifications of an FFR scheme into account in its design for optimal performance is presented. The FFR scheme, termed EFCC, is a wide-area monitoring and control system, which uses synchronized measurements from Phasor Measurement Units (PMUs) to detect network disturbances and instruct fast and coordinated responses from a variety of controllable resources (e.g. wind, demand, energy storage, etc.) [5].

An overview of the EFCC scheme is illustrated in Fig. 9. The system uses a distributed control mechanism, which is considered to have a number of compelling advantages compared to a centralised control scheme including:

- A fully centralised scheme is considered to be prohibitively intensive on the communication network, while the distributed control scheme can be designed with predictable latency and the quantity of data being sent across the wide-area network can be minimised through the use of aggregation.
- The control decision made at the resource side minimises the latency on the transmitted control signal, therefore allowing for better coordination among various controllers in the scheme.
- There is no single point of failure, therefore providing graceful degradation in the scheme.

The EFCC scheme contains three main components, i.e. Central Supervisor (CS), Regional Aggregator (RA) and Local Controller (LC). The transmission network is divided into a number of regions, and each region is a generator-coherency group, i.e. a part of the network with generators whose frequencies are closely tied together during disturbances. The entire system has one CS; each region of the network has one RA and each resource providing the FFR has one LC.

PMUs are installed across the network for real-time measurement of phase, frequency and RoCoF. The measured data is aggregated and processed at regional levels by the RAs and fed to all LCs. When a frequency disturbance occurs, the LCs detect the event based on the real-time measured and processed data, and calculate the total response required for the whole network and also the regional response required for different parts of the network based on the regional impact of the disturbance. The CS monitors the resource availability information across the network and the available resources are coordinated and optimized considering its ramp-up rate, capacity and response delay as discussed in Section 3. Each region will have a targeted amount of response and an optimized sequence for available resources to be deployed, based on which the regional, fast frequency response is instructed.

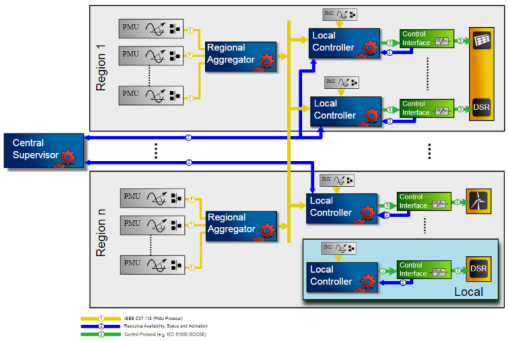

Fig. 9. Schematic of the EFCC scheme

4.1. Central Supervisor (CS)

The CS performs a coordination role for the resources providing FFR. It collects the live resource information from the system and performs continuous analysis on the available resources to identify the optimal resources to achieve the fastest frequency response. This optimisation function assigns a priority to each of the resources that are available and issues a summary of the results down to each of the LCs. The CS does not make any real-time control decisions.

4.2. Regional Aggregators (RAs)

In each region of the network, there will be a number of PMUs installed to capture the frequency and voltage phasor information. Each region is equipped with an RA, which performs two key functions: data aggregation and averaging. The RAs combine the frequency and angle information from PMUs installed in the corresponding region to produce a single aggregated regional 'equivalent' frequency and angle signal to represent that region. This aggregated data is broadcast on the communications network, where all LCs would subscribe to the data streams. By combining the individual signals into aggregated signals, the amount of data that is broadcast on the communications networks is significantly reduced, thereby reducing the bandwidth requirements for the scheme.

4.3. Local Controllers (LCs)

The LCs are the real-time monitoring and control decision making elements. Each FFR service provider (e.g. energy storage units) in the system is equipped with an LC, which receives the data broadcast by all RAs, i.e. the LCs have visibility of signals from all the other regions. The regionally aggregated signals from RAs are used by the LCs to perform a further level of aggregation, which produces a system equivalent frequency and RoCoF. The system equivalent quantities are used to determine whether a frequency event has

occurred and avoid mal-detection of non-frequency events (e.g. faults) due to local measurement.

Through comparison of the regional signals with the system equivalent quantities, the LCs can then determine which regions are most affected by the current event, thereby providing the locational consideration of the control scheme. Each LC makes this assessment autonomously; therefore, loss of a single controller does not prevent the overall control scheme from acting. Furthermore, as each LC is subscribed to the same set of wide-area aggregated data, it will make the same event detection determination.

When an event occurs, every LC uses the information received from the CS to identify whether it is required to respond and how much power it should respond to the current event. The LC will then continuously monitor the frequency behaviour to determine if more response is required. When the frequency and RoCoF have stabilised, the LCs will start to release the requests from their resources. This controlled reduction of the fast frequency response makes way for the traditional primary response to act, which will then restore the frequency.

5. Case study

5.1. Test setup

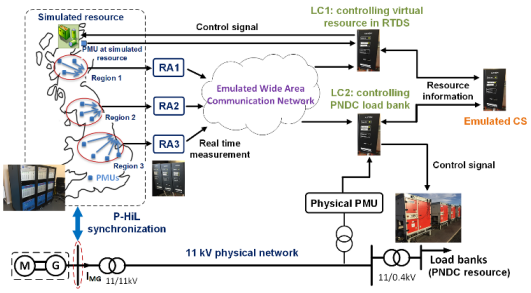

Fig. 10. Test setup for validation of the EFCC scheme

A flexible and realistic testbed, as shown in Fig. 10, has been established at the Power Network Demonstrator Centre (PNDC) for comprehensive validation of the EFCC scheme [12]. In this setup, three RAs and two LCs are tested. The function of the CS is emulated using a dedicated software block. The testbed contains two main parts: a reduced GB transmission network simulated in a real-time digital simulator (RTDS) and an 11 kV physical network with load banks connected. The simulated GB transmission network model is coupled with the 11 kV physical network through a Power-Hardware-in-the-Loop (P-HiL) setup using a MW scale Motor-Generator set .

The simulated network model in RTDS is divided into three regions and PMU models are installed across the network, streaming real-time synchrophasor data to the three RAs. The three RAs receive and process real-time measurements from the RTDS virtual PMUs and send data to the two LCs. One LC (LC_1) controls an energy storage resource modelled in RTDS and the other LC (LC_2) controls the physical load bank at PNDC acting as demand side response. In addition to the PMUs installed across the network, each LC is equipped with one local PMU for local measurement, which is used in case of failure in receiving good quality wide area monitoring signals. The local PMU used by LC_2 is a physical PMU installed at the PNDC network, while LC_1 uses a modelled PMU in RTDS.

The emulated CS has knowledge of the resource availability information from two resources controlled by LC_1 and LC_2 and it sends the information to two LCs, which is used to determine the amount of resource required during a frequency disturbance.

5.2. Test case

The EFCC scheme is being tested under a wide range of network conditions and disturbances including frequency and non-frequency (e.g. faults without loss of generation) events. The tests also involve degrading the communication system performance using a communications emulator to investigate the impact of the communication issues on the EFCC scheme.

In this test case, a loss of generation event is used to illustrate the operation of the EFCC scheme. The event occurs in the north part of the system, i.e. in Region 1, where LC_1 is located. The size of the event is an instantaneous loss of 1 GW of generation. The capacities of the resources at LC_1 and LC_2 are 200 MW and 100 MW respectively; the energy storage resource at LC_1 is modelled using a current source, so it can deliver power instantaneously following a command; for the load bank controlled by LC_2, the time taken to achieve the required power is also negligible, but it is subject to up to 1 s of delay resulted from the load bank's proprietary controller, which only updates the load level approximately every 1 s.

5.3. Test results

The test results from the event are shown in Fig. 11. The first plot shows the aggregated overall system frequency during the event. The second plot shows the RoCoF measured by the two LCs using both wide-area and local real-time data. The third plot indicates the event detection signal from two LCs. This signal will become high when the LCs detect a frequency event in the network. The last plot shows the commands sent by the LCs to request power to respond to the frequency event.

It can be seen from the Fig. 11 that the loss of generation event occurs at around 24.5 s, which is detected by both LCs at around 25 s. Fig. 12 shows the frequency measurements at the three RAs, and it can be clearly seen that there is regional variation in frequency. Region 1, which is closest to the event, is firstly affected with the largest initial drop in frequency. Following that, the frequency measured at Region 2 and 3 also decreases and the frequency at the three regions starts to oscillate.

In Fig. 11, it can be seen that LC_1, which is closest to the event, requested its full power immediately after the event is detected. As discussed previously, this is due to the fact that Region 1 is most severely affected by the event. This control action aims to minimise the regional variation in frequency and the angle separation. This is evident by the results in Fig. 11, where the frequency oscillation dampens following the LC_1's response. LC_2 has a delay in responding to this event. It is considered that this is to avoid stressing the angle separation during the event. Fig. 13 shows the comparison of the frequency behaviour with and without the EFCC fast frequency

response. It can be seen that only with 300 MW of EFCC response, the frequency behaviour has been clearly improved.

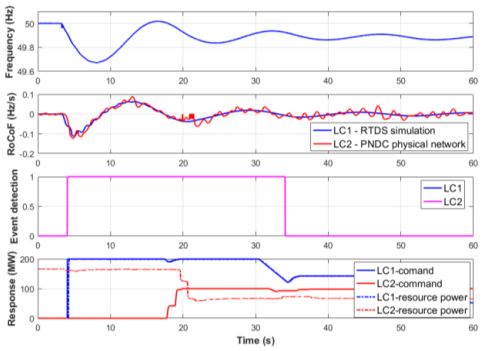

Fig. 11. Test results from the LCs

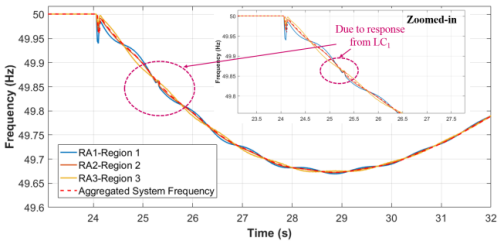

Fig. 12. Measurement data in RAs during the event

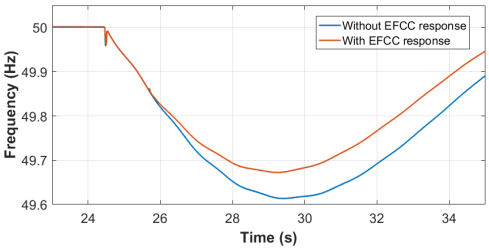

Fig. 13. Comparison of frequency behaviour with and without EFCC scheme

4 Conclusions

This paper has investigated the potential of using FFR to facilitate frequency control in a power system with low inertia. A GSFR model has been developed to demonstrate that reduced system inertia will lead to a faster frequency drop and lower frequency nadir for the same amount of power imbalance, and a significantly larger amount of available primary response reserve is required to maintain the frequency at an acceptable level. FFR is shown to be an effective solution in facilitating the frequency control and it allows the frequency to be maintained within the required limit with much lower reserve and therefore lower operational cost.

The impact of the characteristics of the resources providing FFR has been investigated in detail. It was found that, while the response time and the total capacity of the resource will affect the overall frequency behaviour, the ramp up rate of the resource is the dominating factor. Short response time and large capacity of the FFR will only be effective when a high ramp up rate can be achieved, otherwise the performance in enhancing frequency control will be largely compromised. This dictates the need for resources other than synchronous generation, e.g. energy storage, demand side resources HVDC interconnectors, etc., to participate in this FFR service.

The paper also presented the EFCC scheme, which is a wide-area monitoring and control system, taking all the desirable specifications of the FFR scheme presented in this paper into account in its design for optimal performance. The design and operation of the EFCC scheme has been presented, along with a case study, which demonstrates that the EFCC scheme is capable of detecting a frequency event in a timely manner and deploying resources with consideration of regional variation of frequency behaviour. The results show that frequency behaviour has been improved with the EFCC fast response. Future work will involve comprehensive validation of the EFCC scheme under a wide range of disturbances and different communication system performance scenarios.

5 Acknowledgements

This work is supported by the GB transmission network operator National Grid under Ofgem's Network Innovation Competition framework.

6 References

[1] National Grid, "System Operability Framework," 2016.
[2] National Grid, "System Needs and Product Strategy," 2017.
[3] P. Kundur, *Power System Stability and Control*: McGraw-Hill Inc., 1994.
[4] "National Electricity Transmission System Security and Quality of Supply Standard," 2017.
[5] P. Wall, N. Shams, V. Terzija, V. Hamidi, *et al.*, "Smart frequency control for the future GB power system," in *IEEE PES ISGT Europe*, 2016.
[6] P. Anderson and M. Mirheydar, "A low-order system frequency response model," *IEEE Transactions on Power Systems*, vol. 5, pp. 720-729, 1990.
[7] P. Ashton, C. Saunders, G. Taylor, A. Carter, et al., "Inertia Estimation of the GB Power System Using Synchrophasor Measurements," *IEEE Transactions on Power Systems*, vol. 30, pp. 701-709, 2015.
[8] *Balancing Mechanism Reporting Service*, 30 Apr 2018, Available: https://www.bmreports.com/
[9] UK Energy Research Centre, "UKERC Energy Supply Theme Synthesis Report," 2014.
[10] National Grid, "National Electricity Transmission System Security and Quality of Supply Standard," 2017.
[11] D. Wilson, S. Clark, S. Norris, J. Yu, *et al.*, "Advances in Wide Area Monitoring and Control to address Emerging Requirements related to Inertia, Stability and Power Transfer in the GB Power System," CIGRE Paris Session, 2016.
[12] C. Booth, F. Coffele, and G. Burt, "The Power Networks Demonstration Centre: An environment for accelerated testing, demonstration and validation of existing and novel protection and automation systems," in *Developments in Power System Protection (DPSP 2014), 12th IET International Conference on*, 2014, pp. 1-6.